EUROPEAN ORGANIZATION FOR NUCLEAR RESEARCH

Addendum to the ISOLDE and Neutron Time-of-Flight Committee

IS490: Seeking the onset of collectivity in neutron-rich krypton isotopes with the mass spectrometer ISOLTRAP

June 1, 2016

V. Manea[1], D. Atanasov[2], K. Blaum[2], B. Cakirli[3], P. Delahaye[4], S. George[2], F. Herfurth[5], A. Herlert[6], M. Kowalska[1], P. van Isacker[4], D. Lunney[7], M. Mougeot[7], D. Neidherr[5], M. Rosenbusch[8], L. Schweikhard[8], A. Shornikov[4], A. Welker[9], F. Wienholtz[1,8], R. N. Wolf[2], K. Zuber[9]

[1] *CERN, Geneva, Switzerland*
[2] *Max Planck Institute for Nuclear Physics, Heidelberg, Germany*
[3] *University of Istanbul, Faculty of Physics, Istanbul, Turkey*
[4] *GANIL, Caen, France*
[5] *GSI Helmholtzzentrum für Schwerionenforschung GmbH, Darmstadt, Germany*
[6] *FAIR, Darmstadt, Germany*
[7] *CSNSM-IN2P3-CNRS, Université Paris-Sud, Orsay, France*
[8] *Ernst-Moritz-Arndt-University, Greifswald, Germany*
[9] *Technical University, Dresden, Germany*

Spokesperson: David Lunney, david.lunney@csnsm.in2p3.fr
Contact person: Vladimir Manea, vladimir.manea@cern.ch

Abstract:

We propose to measure the masses of neutron-rich krypton isotopes $^{98-100}$Kr, using the versatile mass spectrometer ISOLTRAP. The proposed masses would extend the evolution of two-neutron separation energies up to neutron number $N = 64$ and thus illustrate the shape-coexistence picture in the neutron-rich nuclei of mass $A \approx 100$ towards the lower-Z boundary. Krypton appears to delimit the onset of collectivity emerging at $N = 60$ in the isotopic chains with larger proton number [1], but the question remains whether the transition observed in the other chains is absent completely or simply shifted to higher neutron number. Neutron-rich krypton isotopes are an important reference for the predictions of density-functional-type models, as well as a fertile testing ground for the role of beyond-mean-field correlation in the description of atomic nuclei. Additionally, studying the neutron-rich krypton isotopes would combine the most recent advances in beam production, purification and measurement at ISOLDE, making ^{100}Kr a highlight case for demonstrating the improved capabilities of the ISOLDE facility.

Requested shifts: 15 shifts of neutron-rich krypton beams from a nano-structured UC_x target with a VADIS ion source and possibly a neutron converter.

1 Motivation

With respect to the evolution of nuclear structure from closed-shell to collective behavior, the neutron-rich nuclides of mass $A \approx 100$ form one of the most prominent regions of the nuclear chart. Mean-square charge radii along the isotopic chains of rubidium ($Z = 37$) to zirconium ($Z = 40$) [2–9] show a gradual increase with neutron number until $N = 60$, where a jump to higher values suddenly takes place (see Fig. 1(a)). At the same location, the two-neutron separation energies S_{2N} [10] start increasing, with a maximum being reached at $N = 61$ (see Fig. 1(b)). Moreover, in even-even nuclei (zirconium and strontium) the excitation energies of the first 2^+ states are suddenly reduced at $N = 60$, while the ratio between the excitation energies of the first 4^+ and 2^+ states approaches the rigid-rotor limit ($3\frac{1}{3}$) [11]. Concomitantly, an excited 0^+ state decreases in excitation energy towards $N = 60$ and then increases at $N = 62$ [11].

The krypton isotopic chain seems to delimit this series of observations, as also observed in Fig. 1, with the trends of S_{2N} [1] and $\delta\langle r^2\rangle$ [2] evolving smoothly up to $N = 61$ and $N = 60$, respectively. A relatively high energy of the first excited 2^+ state was determined for ^{96}Kr (554 keV [12]) with respect to its $N = 60$ isotone ^{98}Sr (144 keV [11]).

Self-consistent mean-field calculations using the Gogny D1S interaction [13, 14] reveal a picture of shape coexistence, in which the nucleus possesses both oblate and prolate intrinsic shapes, in competition for the ground-state configuration. In a static approximation in which the ground state is assigned to the intrinsic shape of lowest energy, they show that the nuclei with $N < 60$ have slightly oblate deformation in the ground state, while around $N = 60$ a transition to prolate deformation occurs. Given the larger deformation of the intrinsic prolate shape, this transition offers the right trend of mean-square charge radii around $N = 60$. However, the evolution of two-neutron separation energies across $N = 60$ does not show the pronounced increase observed in experiment.

Mean-field calculations Fig. 1 using the Skyrme SLy4 interaction show a similar shape-coexistence and shape-transition picture [15]. Additionally, they reveal that the same prolate and oblate shapes are also present around $N = 60$ in the krypton isotopic chain, but, unlike for the higher-Z chains, the energy difference between the two configurations is very small [15, 16]. The systematic studies of [15, 16] also show that the binding-energy difference between them depends on the pairing interaction. In particular, pairing-interaction values which allow a pronounced-enough effect in the S_{2N} values at $N = 60$ also determine an oblate-to-prolate transition to occur in the krypton isotopic chain for higher neutron number than what has been so far investigated experimentally. In Fig. 1 this determines a change of trend to occur both in the $\delta\langle r^2\rangle$ and S_{2N} values of krypton isotopes.

The existence of such a transition or its consequences on the ground-state observables depends on the employed theoretical framework. Figure 2 shows the experimental $\delta\langle r^2\rangle$ and S_{2N} values in the region of interest, compared to predictions of various models using state-of-the-art energy density functionals [17–20] (represented for the even-even krypton and strontium isotopes). One notices that the three functionals give a similar description of the S_{2N} and $\delta\langle r^2\rangle$ for the strontium isotopic chain, but the SLy4 functional predicts a slightly different evolution of the two observables for the krypton isotopes.

Apart from the differences occurring between the predictions of the different calculations

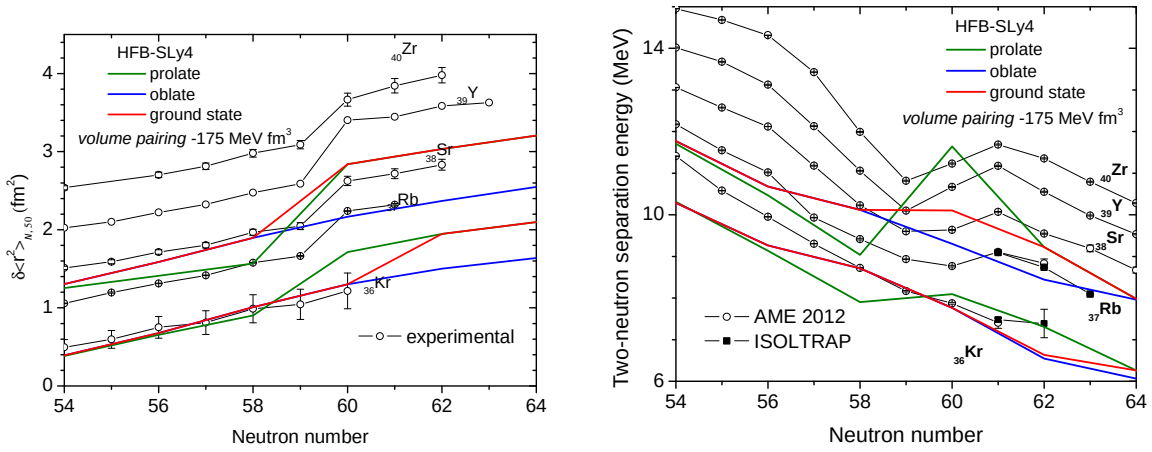

(a) (b)

Figure 1: Experimental mean-square charge radii (a) [2–9] and two-neutron separation energies (b) [10,15] of neutron-rich $A \approx 100$ nuclei, compared to mean-field calculations using the Skyrme SLy4 interaction [16], for the even-even krypton and strontium isotopes. The calculations present separately the trends corresponding to the oblate and prolate configurations, as well as the resulting trend for the ground state, when assigned to the configuration of lowest energy. Mean-square charge radii are represented as displacements to the corresponding $N = 50$ isotope.

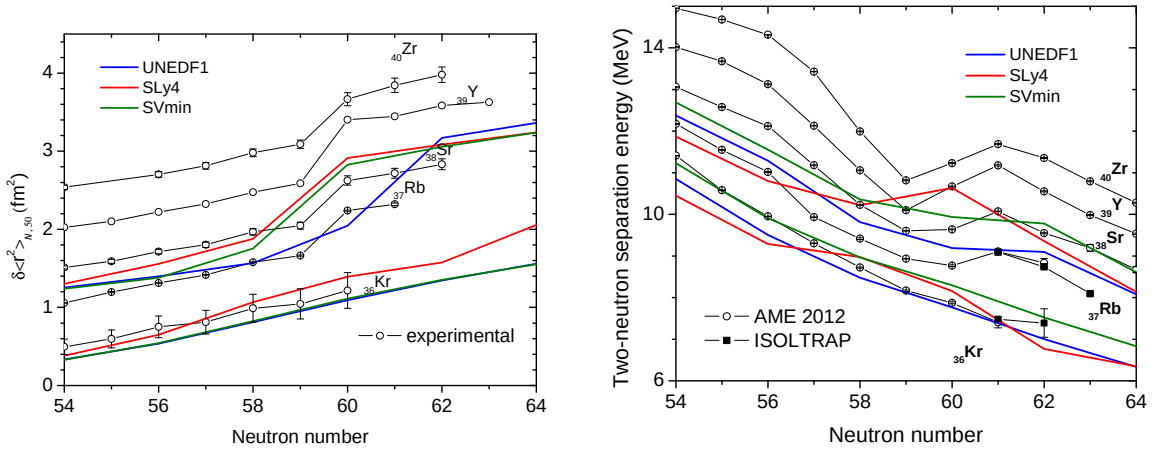

(a) (b)

Figure 2: Experimental mean-square charge radii (a) [2–9] and two-neutron separation energies (b) [10,15] of neutron-rich $A \approx 100$ nuclei, compared to calculations using state-of-the-art nuclear density functionals [17] ([18] in blue , [19] in red and [20] in green).

when treating shape coexistence in the mean-field approximation, recent calculations of even-even krypton isotopes using the Gogny D1S interaction [21] show that triaxiality and beyond-mean-field configuration mixing might play a significant role in correctly describing the properties of the nuclei in the region. Still, ^{98}Kr is predicted to have a structure in which the oblate and prolate configurations are not mixed, the former being

the dominant configuration for the ground-state band and the latter corresponding to an excited 0^+ state. A weak mixing between the two configurations in the ground state was also observed in a recent study of ^{98}Sr [22]. This means that the simple mean-field competition picture is not completely washed out by beyond-mean-field correlations and the change in the predominant configuration of the ground state might be well reflected in the trend of binding energies. Given that the effect might be weaker than in the strontium isotopic chain, high-precision mass measurements are required to pin down the structure of krypton isotopes.
In this proposal we would thus like to continue the measurements of masses of krypton isotopes beyond $N = 61$, in order to investigate whether a sudden change of structure still takes place in the nuclear ground state with the addition of neutrons to the system. Together with the strength of the transition at $N = 60$ in the isotopic chains with larger proton number, the presence of a transition or absence thereof in the krypton isotopic chain would weight significantly in the optimization of state-of-the-art mean-field or density-functional-type approaches, as well as for understanding the beyond-mean-field configuration mixing of the intrinsic shapes in the region.

2 Experimental setup

The proposed measurements will be performed using the mass spectrometer ISOLTRAP [23]. As shown in a recent review [24], the current ISOLTRAP experiment consists of a linear radio-frequency quadrupole (RFQ) cooler and buncher, a multi-reflection time-of-flight mass spectrometer (MR-TOF MS) and two Penning traps, one for ion-bunch preparation and one for precision mass spectrometry. The MR-TOF MS can be used either as beam purifier [25] or mass spectrometer [26], being a complementary approach to Penning-trap mass spectrometry for very weak or short-lived isotopes (half-lives in the 10-100 ms range and yield below 10 ions per μC). It also allows the on-line analysis of the beam composition and optimization of the beam production parameters (target-ion-source conditions, synchronization to release time structure, beam preparation). The relative precision achievable with the MR-TOF MS is close to 10^{-7}, sufficient for answering the question of the structure of neutron-rich krypton isotopes. In the case of beams intense enough to be measured with the precision Penning trap (which typically means yields above 10^2 ions per μC and half-lives larger than 50 ms), the MR-TOF MS would additionally offer an independent determination of the mass value.

3 Beam-time request

Krypton isotopes were observed at ISOLTRAP in 2015 at the end of a scheduled IS490 experiment which was dedicated to neutron-rich argon isotopes. The experiment used a standard uranium carbide target and a VADIS ion source [27]. The mass of ^{97}Kr was determined using the precision Penning trap (the 2010 measurement was achieved by a buffer-gas cooling resonance using the preparation trap [1]) and the mass of ^{98}Kr was measured for the first time, using the MR-TOF MS. The spectrum of $A = 98$ isobars detected after the MR-TOF MS is presented in Fig. 3. One notices that, despite the

dominant contribution of the doubly charged ^{186}Hg, the ^{98}Kr peak is clearly separated. The results from the mass measurements performed in 2015 are included in Figs. 1 and 2. One notices that the achieved precision for ^{98}Kr is not sufficient to constrain the trend of the two-neutron separation energies beyond $N = 61$. This is due to the limited time that was available to accumulate sufficient statistics.

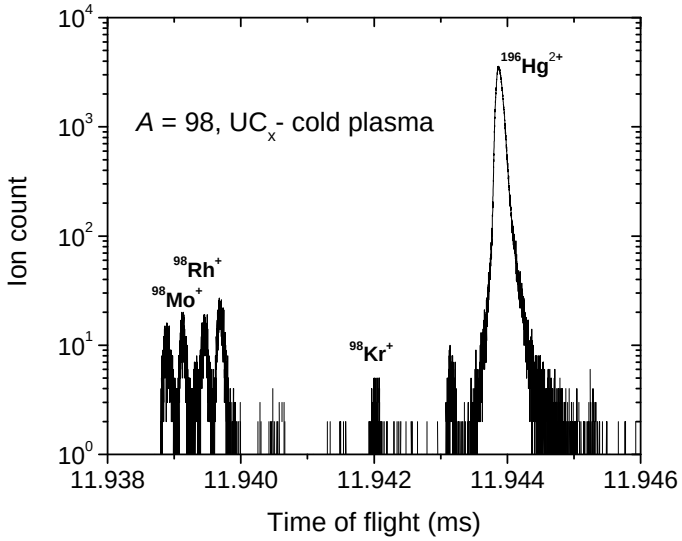

Figure 3: Time-of-flight spectrum of $A = 98$ isobars observed behind the MR-TOF MS in 2015, produced using a uranium carbide target with a VADIS ion source and a cooled transfer line.

Detailed shift request

The table below presents the detailed request of shifts of radioactive beam for the krypton isotopes, as well as the ISOLDE database yields obtained with a standard cooled-line plasma source and protons shot directly on the target [28]. The low yield of ^{100}Kr from [28] makes it an excellent example to demonstrate the developments in beam production and measurement taking place at ISOLDE during the last decade. The use of the new nano-structured uranium target material could significantly enhance the release properties of krypton isotopes and hence bring the ^{100}Kr yield closer to the in-target production rate of 100/μC [28]. Another enhancement in production efficiency could be achieved by using the new VADIS for the ionization of the krypton isotopes, with optimized operation parameters [27]. To circumvent possible contamination from doubly charged mercury, the target unit could be equipped with a neutron converter. A 30% efficiency for production with neutron converted is estimated in [28], which is acceptable if the contamination can be dramatically suppressed. The use of a neutron converter with optimized geometry would however enhance the efficiency even more. All these new techniques and developments in ion-beam production would be combined with the high sensitivity of the MR-TOF MS, thus allowing, aside from the study of the krypton isotopes, a direct characterization of their performance.
In order to perform all required tests and optimizations for ion production, we request 2

additional shifts.
The number of requested shifts includes the time required for setting-up the measurement cycle of ISOLTRAP and for the identification in the precision Penning trap of reference isobars for MR-TOF mass measurements (typically one shift for each isotope).

Isotope	Half-life (ms) [29]	Yield [28](μC^{-1})	Target/ion source	Method	Shifts (8h)
^{98}Kr	42.8(3.6)	470	UC_x/VADIS (cooled line)	Penning trap and MR-TOF MS	3
^{99}Kr	40(11)	9	UC_x/VADIS (cooled line)	MR-TOF MS	4
^{100}Kr	12(8)	< 1	UC_x/VADIS (cooled line)	MR-TOF MS	6
				Target-ion source optimization:	2
				Total shifts:	**15**

Summary of requested shifts: 15 shifts of neutron-rich krypton beams from a nano-structured UC_x target, possibly with neutron converter and a VADIS ion source.

References

[1] S. Naimi, *et al.*, *Phys. Rev. Lett.* **105**, 032502 (2010).

[2] M. Keim, *et al.*, *Nucl. Phys. A* **586**(2), 219 (1995).

[3] C. Thibault, *et al.*, *Phys. Rev. C* **23**, 2720 (1981).

[4] F. Buchinger, *et al.*, *Phys. Rev. C* **41**, 2883 (1990).

[5] P. Lievens, *et al.*, *Phys. Lett. B* **256**(2), 141 (1991).

[6] B. Cheal, *et al.*, *Phys. Lett. B* **645**(23), 133 (2007).

[7] P. Campbell, J. Billowes, I. S. Grant, *J. Phys. B* **30**(21), 4783 (1997).

[8] P. Campbell, *et al.*, *Phys. Rev. Lett.* **89**, 082501 (2002).

[9] H. L. Thayer, *et al.*, *J. Phys. G* **29**(9), 2247 (2003).

[10] M. Wang, *et al.*, *Chinese Phys. C* **36**, 1603 (2012).

[11] M. Bhat, in S. Qaim (ed.), *Nuclear Data for Science and Technology*, Research Reports in Physics, pp. 817–821. Springer Berlin Heidelberg (1992), Data extracted using the NNDC On-Line Data Service from the ENSDF database (http://nndc.bnl.gov), file revised as of 1.06.2016.

[12] M. Albers, *et al.*, *Phys. Rev. Lett.* **108**, 062701 (2012).

[13] R. Rodríguez-Guzmán, P. Sarriguren, L. M. Robledo, *Phys. Rev. C* **82**, 061302 (2010).

[14] R. Rodríguez-Guzmán, P. Sarriguren, L. Robledo, S. Perez-Martin, *Phys. Lett. B* **691**(4), 202 (2010).

[15] V. Manea, *et al.*, *Phys. Rev. C* **88**, 054322 (2013).

[16] V. Manea, *Penning-trap mass measurements of exotic rubidium and gold isotopes for a mean-field study of pairing and quadrupole correlations*, Ph.D. thesis, Université Paris-Sud XI, Orsay, France (2014).

[17] J. Erler, *et al.*, *Nature* **486**(7404), 509 (2012).

[18] M. Kortelainen, *et al.*, *Phys. Rev. C* **85**, 024304 (2012).

[19] E. Chabanat, P. Bonche, P. Haensel, J. Meyer, R. Schaeffer, *Nucl. Phys. A* **635**(12), 231 (1998).

[20] P. Klüpfel, P.-G. Reinhard, T. J. Bürvenich, J. A. Maruhn, *Phys. Rev. C* **79**, 034310 (2009).

[21] T. R. Rodríguez, *Phys. Rev. C* **90**, 034306 (2014).

[22] E. Clément, *et al.*, *Phys. Rev. Lett.* **116**, 022701 (2016).

[23] M. Mukherjee, *et al.*, *Eur. Phys. J. A* **35**, 1 (2008).

[24] S. Kreim, *et al.*, *Nucl. Instrum. Meth. B* **317**, 492 (2013).

[25] R. Wolf, *et al.*, *Nucl. Instrum. Meth. A* **686**, 82 (2012).

[26] R. Wolf, *et al.*, *Int. J. Mass Spectrom.* **349–350**, 123 (2013).

[27] L. Penescu, R. Catherall, J. Lettry, T. Stora, *Rev. Sci. Instrum.* **81**(2), 02A906 (2010).

[28] U. Bergmann, *et al.*, *Nucl. Instrum. Meth. B* **204**, 220 (2003).

[29] G. Audi, *et al.*, *Chinese Phys. C* **36**(12), 1157 (2012).

Appendix

DESCRIPTION OF THE PROPOSED EXPERIMENT

The experimental setup comprises: ISOLDE central beam line and ISOLTRAP setup. The ISOLTRAP setup has safety clearance, the memorandum document 1242456 ver.1 "Safety clearance for the operation of the ISOLTRAP experiment" by HSE Unit is released and can be found via the following link: https://edms.cern.ch/document/1242456/1.

Part of the	Availability	Design and manufacturing
ISOLTRAP setup	☒ Existing	☒ To be used without any modification